2006

Inter-layer distance optimisation for a light-based flowmeter by means of CFD

Ajit Godbole
University of Wollongong, agodbole@uow.edu.au

Buyung Kosasih
University of Wollongong, buyung@uow.edu.au

Anton Fuchs
Graz University of Technology

Publication Details

Godbole, A., Kosasih, B. & Fuchs, A. (2006). Inter-layer distance optimisation for a light-based flowmeter by means of CFD. 2006 AIChE Spring National Meeting - 5th World Congress on Particle Technology (pp. 1-9).

Inter-Layer Distance Optimisation for a Light-Based Flowmeter by Means of CFD

Ajit Godbole[1], Buyung Kosasih[1] and Anton Fuchs[2]

[1] School of Mechanical, Materials and Mechatronics Engineering, University of Wollongong, AUSTRALIA

[2] Institute of Electrical Measurement and Measurement Signal Processing, Graz University of Technology, AUSTRIA

ABSTRACT

A non-intrusive method to measure the particle velocities in dilute-phase pneumatic conveying is described. The method is based on correlating signals, which are measured in two flow cross-sections. The cross-correlation function generated provides information about the time it takes for a particle to travel between the measurement planes. Knowing the inter-plane distance and the time delay, the particle velocity can be calculated. The two measurement planes must be an optimum distance apart to ensure the best possible signal resolution and sufficient quality of the cross-correlation: If the distance is too small, the resolution is coarse, while for a too large distance, the pipe contents in the two cross-sections may differ due to curved particle trajectories (e.g. due to gravity), leading to weak cross-correlation functions.

In this paper, experimental measurements and Computational Fluid Dynamics (CFD) simulations of dilute-phase pneumatic conveying processes are reported. Particle trajectories for a given pipe geometry and different conveying velocities are used to estimate an optimal inter-layer distance.

KEYWORDS: Computational Fluid Dynamics, Particle Trajectories, Flowmeter, Cross-Correlation Function

I. INTRODUCTION

Flow determination and observation of granular flow have become an important task in many industrial conveying processes. Especially for dilute phase granular flow, determination of particle velocities and velocity profiles is crucial for an appropriate dimensioning of conveyor systems and for safe conveying with minimum damage to the conveyor pipe and the conveyed material. Abrasive material conveyed at high velocities and unpredictable fluctuations in flow properties make a non-invasive measurement principle with on-line velocity determination desirable [1]. Optical non-invasive approaches to determine granular material flow, such as Laser Doppler Velocimetry (LDV) [2], and Particle Image Velocimetry (PIV) [3], have been used.

Cross-correlation flowmeters work on a different principle: Properties of the material flow are measured in two flow cross-sections separated by a certain distance. Natural or artificial fluctuations in the flow are detected and signals from the two layers are correlated [4]. The measured quantity may be electrical charge, electrical capacitance, light attenuation, γ-radiation or acoustic noise [5]. In this paper, application of the light attenuation technique is described.

The cross-correlation function (CCF) Φ_{12} of signals from the two planes is defined by:

$$\Phi_{12}(\tau) = \lim_{T\to\infty} \frac{1}{T} \int_0^T x_1(t).x_2(t-\tau)dt \quad (1)$$

where x_1 and x_2 are the time-dependent signals from the two measurement planes respectively, τ is the time delay and T the integration time.

An infinite velocity of particles with axis-parallel trajectories would result in two identical signals in both planes and hence in a CCF with a maximum exactly at the centre position (no time delay between the two signals). Since the particle velocity is finite, the time delay in the signals and hence the shift of the peak in the CCF function is a measure of the particle velocity.

When the maximum in the CCF is found for the time delay τ^*, the particle velocity v_p can be obtained by:

$$v_p = d_{12} / \tau^* \quad (2)$$

where d_{12} is the distance between the measurement planes.

II. PNEUMATIC CONVEYING

In dilute-phase granular flow processes, a conveyed particle passing the first measurement plane causes a significant change in the measured signal in this layer. Depending on the conveying velocity, the same particle will appear in the downstream measurement plane after a certain time delay, again causing a significant change in signal form.

Good signal correlation is possible only if the material behaviour is similar in the two measurement planes. For very small distances, the flow appears similar in the two planes. This results in a good match between the two derived signals but a bad resolution for velocity calculation. For larger inter-layer distances and time delays, the resolution is better. But curved particle trajectories, such as due to the omnipresent gravity effect, can cause the flow in the two pipe cross-sections to look different. This results in a weak CCF. The optimum inter-layer distance is a trade-off between reliable CCF and usable resolution for velocity calculation.

'White Plastic Pellets 820', (nearly spherical, average diameter ~3.78 mm, density 925 kg/m^3), were pneumatically conveyed in a 49.9 mm ID horizontal pipe with a sight-glass section 230 mm long. The photograph in Fig. 1 shows that the particle 'loading' was small enough for the process to be classified as 'dilute-phase' pneumatic conveying. The pipe test section was nearly 5 m downstream of the air pump, so that a fully established flow can be assumed. Average air velocities, measured by Pitot-Static tubes, ranged from about 15 m/s to 35 m/s.

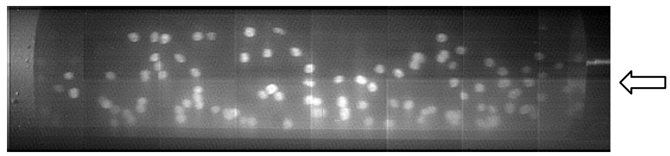

Fig. 1: Pneumatically Conveyed Plastic Pellets

III. MEASUREMENT TECHNIQUE

Two banks of six Light Dependent Resistors (LDRs) were used to test the cross-correlation principle for several inter-layer distances. The use of *multiple* sensors enables determination of particle velocity *profiles*. The LDRs are mounted on the glass pipe wall, and illuminated from the opposite side. Corresponding LDRs in the two layers are at the same height. The sensitive volume for each sensor is shown schematically in Fig. 2 as a cylinder perpendicular to the flow.

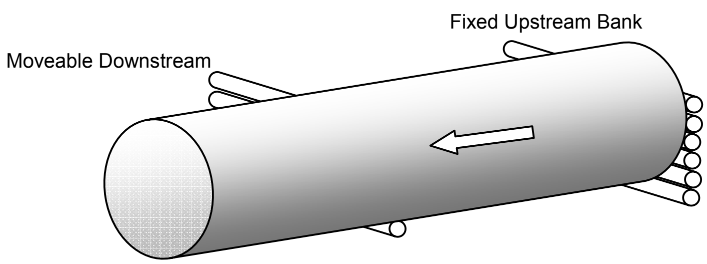

Fig. 2: Two banks with six LDR sensors each

Each sensitive cylinder is 4.5 mm in diameter. The best cross-correlation is achieved when the same particle casts a similar shadow on the corresponding LDRs, as it flies past one, then the next. When this happens, there is a similar *change* in the electrical resistances of the corresponding LDRs, and a strong peak in the CCF. When this does not happen, weak cross-correlation results. In the present experiment, in general, for a particle deviation of more than 4.5 mm, the signals have no similarity and the cross-correlation principle will fail for this particle (Fig. 3).

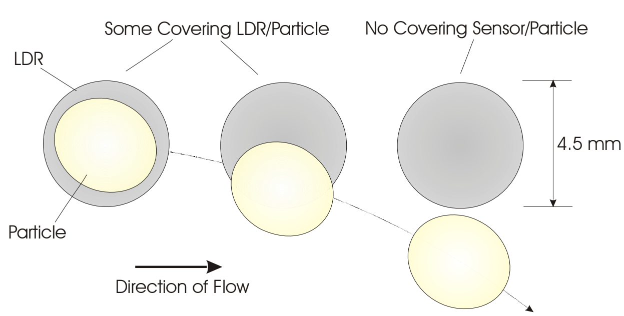

Fig. 3: Particle flight across successive LDRs showing decreasing masking between sensitive LDR surface and particle

Thus, it becomes necessary to estimate the extent of particle deviation from a straight flight path over different distances, for different flow conditions.

Recent advances in Computational Fluid Dynamics (CFD) techniques enable tracking the conveyed particles between the measurement planes, for different flow conditions. This suggests the possibility of combining the techniques of CFD and the cross-correlation principle to estimate optimum inter-layer distances for different flow conditions. The following paragraphs explore this possibility.

IV. CFD SIMULATIONS

The steady-state flow simulations were carried out using the CFD package CFX (version 5.7.1).

Computational Domain and Mesh

The flow region of interest is the 230 mm long sight-glass portion of the pipe. This was chosen as the 'computational domain' for the simulation (Fig. 5).

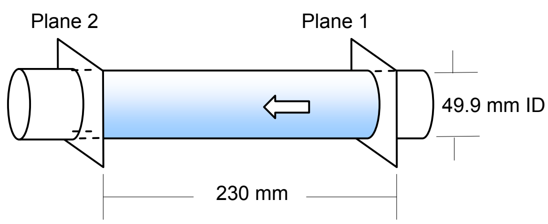

Fig. 5: Chosen computational domain for the CFD simulations

The computational domain is divided into a number of non-overlapping tetrahedral 'cells', forming the computational mesh. These cells are non-uniformly distributed, with denser cell population in regions where steep gradients in the flow parameters are expected, such as the pipe wall (Fig. 6).

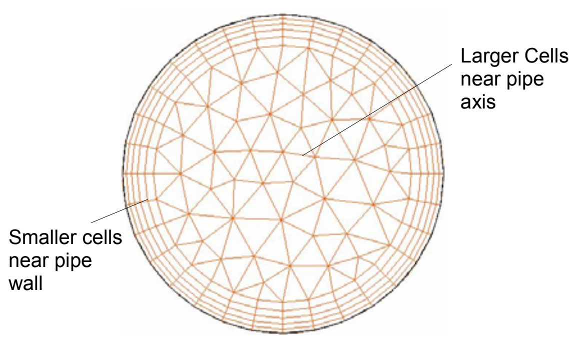

Fig. 6: Non-uniform mesh in pipe cross-section

Simulation Technique

The pipe Reynolds numbers for the experimental velocity range vary from about $4.99(10^4)$ to $1.16(10^5)$. Assuming a transition Reynolds number for pipe flows to be about 2300 [6], this implies a turbulent flow. Partial differential equations expressing continuity and momentum balances, and those for the turbulent kinetic energy and its dissipation rate for the continuous fluid medium are integrated over the volume of each cell to obtain discretised (algebraic) versions. These algebraic equations are solved iteratively until balances are achieved for each cell. Since the cells are contiguous, this implies a balance over the entire computational domain. In the present 'cold flow' simulation, solution of the thermal energy equation is not needed.

Conveying Medium

Air at 25°C is assumed to be the conveying medium. Compressibility effects are assumed negligible.

Particle Tracking

Fully coupled with the motion of the continuous conveying medium, the motion of discrete conveyed particles (mass m_p) is described by Lagrangian equations of the form

$$m_p \frac{d\vec{v}_p}{dt} = \vec{F} \tag{3}$$

where $\vec{v}_p$ is the particle velocity, and $\vec{F}$ the total force acting on it. In the most general case, $\vec{F}$ is composed of various components: viscous drag due to relative motion between particle and fluid, due to pressure gradients in the enveloping fluid, force to accelerate the virtual mass of fluid in the volume occupied by the particle, buoyancy force due to gravity, Bassett force resulting from the previous history of the motion, and centripetal and Coriolis forces. In the present case, the conveyed particles are assumed spherical, and are much denser than the conveying medium. The motion occurs in a non-rotating frame of reference. Under these conditions, the equation of particle motion becomes:

$$\rho_p \frac{\pi d_p^3}{6} \frac{d\vec{v}_p}{dt} = \frac{1}{8}\pi \rho_f d_p^2 C_D \left|v_f - v_0\right|\left(\vec{v}_f - \vec{v}_0\right) + \frac{\pi d_p^3}{6}\left(\rho_p - \rho_f\right) g \tag{4}$$

where ρ_p and ρ_f are particle material density and fluid density respectively, d_p is the particle diameter, and C_D is the particle drag coefficient.

Boundary Conditions

The computational domain is enclosed by three surfaces: Inlet, Outlet, and Wall. A $(1/7)^{th}$ power law velocity profile is assumed for the fully established flow at the inlet [6]. Ten particles are 'injected' at evenly spaced points in the inlet plane. The no-slip wall boundary condition is applied to the pipe wall, and zero gauge pressure condition at the outlet.

Fig. 7 shows typical simulation results. Of the ten tracks shown in Fig. 7a, a single track is isolated in Fig. 7b for comparison with a typical experimentally determined particle track as shown in Fig. 8.

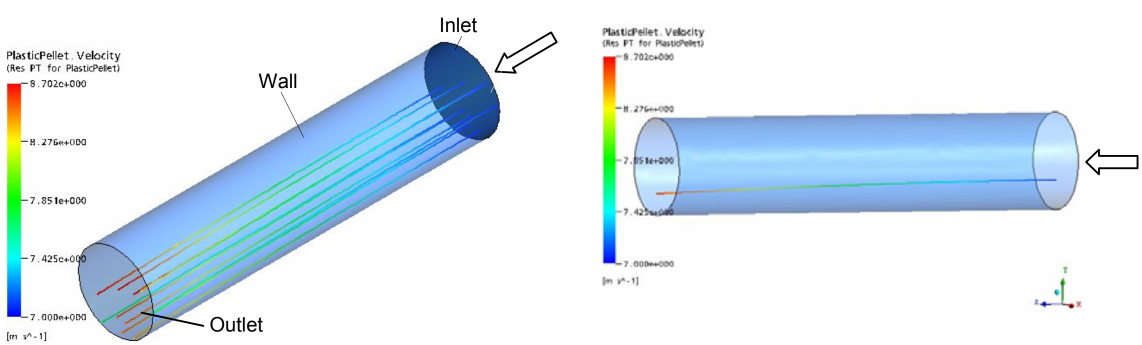

(a) **(b)**

Fig. 7: (a): Typical particle tracks result (ten tracks shown; Inlet velocities: Air velocity 30 m/s; Particle velocity 7 m/s) and (b): Single particle trajectory

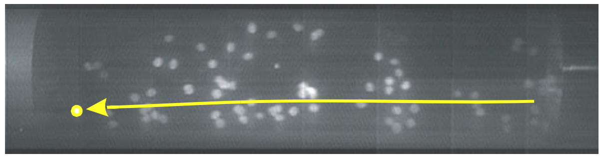

Fig. 8: Typical experimental particle track

Fig. 9 is a typical normalized particle track, showing particle descent vs axial location for a considered pipe length of 230 mm, an air inlet velocity of 30 m/s and a particle inlet velocity of 7 m/s. It can be seen that over the observable distance (length of the sight-glass), the free descent of a typical particle is about 5.3 mm. This agrees very well with experimental observations.

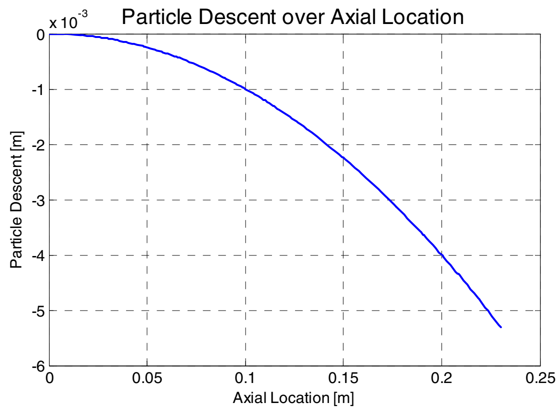

Fig. 9: Typical simulated particle descent (Inlet velocities: Air 30 m/s; Particles 7 m/s)

Parametric Studies

CFD simulations can thus be used to estimate the optimum inter-plane distance for non-intrusive particle velocity measurements. Parametric CFD simulations were carried out in order to provide more general guidelines relevant to dilute-phase pneumatic conveying, for different flow conditions. It was found that the optimum distances are very insensitive to different particle sizes and densities, but very strong functions of the conveying gas velocities. Fig. 10 summarizes these results.

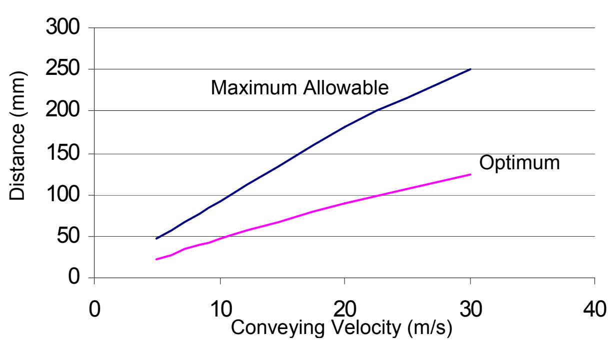

Fig. 10: Maximum allowable and optimum distances as functions of conveying velocity

V. MEASUREMENT RESULTS

A typical particle descent of this magnitude over 230 mm suggests that the LDR measurements plane should certainly be located less than 230 mm apart, for this particular flow condition. In order to test this observation, experiments were carried out for four different inter-plane distances. The CCFs for these measurements are shown in Fig. 11.

It can be seen that the height of the CCF peak decreases for larger distances, since the similarity between the corresponding signals decreases. It can also be seen that the peak becomes increasingly blurred for larger inter-plane distances. On the other hand, the obtained time delays are 21 'ticks' for 40 mm distance, 31 for 60 mm, 40 for 80 mm, and 56 ticks for 100 mm inter-layer distance, resulting in higher resolution corresponding to the increased time delay (the measurement sampling rate was 3906 Hz, so that one 'tick' is equivalent to about 0.256 ms).

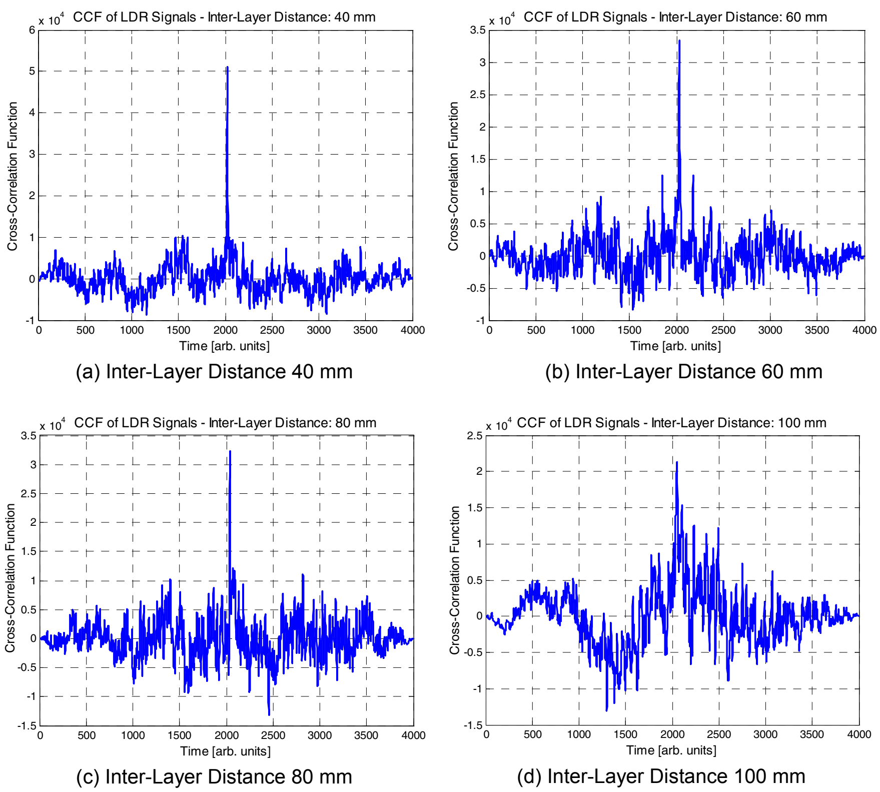

Fig. 11: CCF vs time for four different distances between measurement planes

The optimum distance represents the best possible combination of peak value and resolution. It is seen that the CCF is already blurred for an inter-plane distance of 100 mm, well below the upper bound of about 230 mm suggested by the CFD simulations. Therefore, CCFs for greater inter-plane distances were not obtained.

Of the four plots, which one represents the optimum inter-plane distance? To answer this question, the measurements were compared with respect to signal similarity (represented by the CCF peak value) and resolution (represented by the time delay). Fig. 12 shows the comparison.

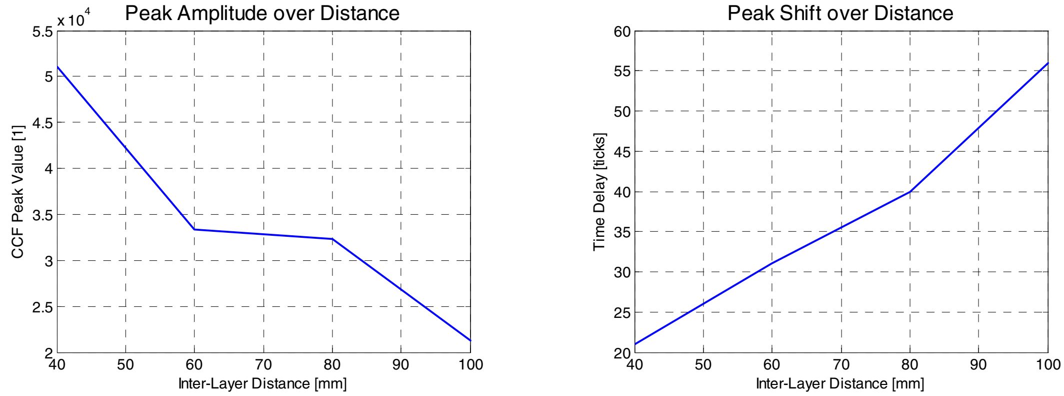

Fig. 12: Signal similarity and time delay vs inter-plane distance

It is seen that while there is a near-linear rise in time delay for progressively greater inter-plane distances, the CCF peak value for the 80 mm distance is not much lower than that for the 60 mm distance. This suggests that the 80 mm distance offers the best compromise between good signal resolution and signal similarity for this flow condition.

Additionally, a semi-automated procedure is used to obtain a velocity vector map for the material flow [7] for an air velocity of about 30 m/s and a particle velocity of about 7 m/s. A high speed camera is used to capture snapshots of the granular dilute phase flow.
First, the camera recording of 312.5 ms duration is divided into 500 individual frames. The white granular particles appear as bright spots in each image (compare Fig. 1). A pattern recognition algorithm is used to identify particles in two consecutive frames and identify pairs of corresponding particles in one image, as shown in Fig. 13. The physical proximity of the two positions of a particle has to be confirmed by the user.

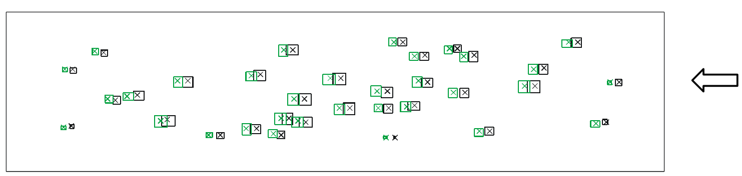

Fig. 13: Identified particles in two consecutive frames

The differences of the particle centres in both positions as well as their absolute coordinates are recorded. Since the time delay Δt between both particle positions and the physical dimension of the pipe geometry are constant and well-known, the particle velocity in flow direction and perpendicular to the flow direction (i.e. ascent or descent of the particles) can be calculated. To avoid multiple information extraction from one particle, that number of frames needed for the slowest particle to move out of the image plane is skipped in the procedure. A mean particle descent of 3.8 mm over a length of 200 mm could be observed, which agrees very well with the CFD simulation results shown in Fig. 9.

VI. CONCLUSION

With a non-intrusive method particle velocities are measured in dilute-phase particle-gas flows in pipes. The estimation of the optimum distance between the upstream and downstream measurement plane is possible using the latest techniques in CFD. This combination of CFD and the cross-correlation measurement principle will be particularly useful in dilute-phase pneumatic conveying processes prevalent in many industries. In this paper, this is demonstrated by calculating the trajectories of conveyed particles. Their simulated descent under the action of gravity is validated against experimental measurements. Parametric simulation studies are carried out to arrive at estimates of the maximum allowable and optimum distances between measurement planes used in the CCF technique.

VII. REFERENCES

[1] J.R. Pugh, The Crucial Role of On-Line Measurement in Bulk Solids Handling, in: Handbook of Conveying and Handling of Particular Solids, A. Levy and H. Kalman (Editors), Elsevier Science, 2001, pp. 793-806.

[2] S.R. Woodhead, A.N. Pittman, S. Ashenden, Laser Doppler Velocimetry Measurements of Particle Velocities in Gas-Solids Two Phase Flows, in: Proc. Instrumentation and Measurement Technology, 1995, pp. 770-773.

[3] M.L. Jakobsen, W.J. Easson, C.A. Greated, D.H. Glass, Particle Image Velocimetry: Simultaneous Two Phase Flow Measurements, in: Measurement Science and Technology, Vol. 7, 1996, pp. 1270-1280.

[4] W.Q. Yang, M.S. Beck, An Intelligent Cross Correlator for Pipeline Flow Velocity Measurement, in: Flow Measurement and Instrumentation, Vol. 8, No. 2, 1997, pp. 77-84.

[5] M.S. Beck, A. Plaskowski, Cross Correlation Flowmeters – Their Design and Application, Adam Hilger, Bristol, 1987.

[6] F.M. White, Fluid Mechanics, McGraw-Hill International Edition 3, 1994.

[7] M. Brandner, A. Fuchs, Model-Based Granular Flow Estimation Using an Array of Low-Cost Transmitted Light Sensors, in: Proceedings of the 4th IEEE Conference on Sensors, Irvine, California, USA, Oct. 31st - Nov. 3rd